JOC The Journal of Organic Chemistry

Article

pubs.acs.org/joc

Doped Polycyclic Aromatic Hydrocarbons as Building Blocks for Nanoelectronics: A Theoretical Study

Pavlo O. Dral,[†] Milan Kivala,*[,‡] and Timothy Clark*[,†]

[†]Computer-Chemie-Centrum and Interdisciplinary Center for Molecular Materials, Department Chemie und Pharmazie, Friedrich-Alexander-Universität Erlangen-Nürnberg, Nägelsbachstrasse 25, 91052 Erlangen, Germany

[‡]Chair I for Organic Chemistry, Department Chemie und Pharmazie, Friedrich-Alexander-Universität Erlangen-Nürnberg, Henkestrasse 42, 91054 Erlangen, Germany

Supporting Information

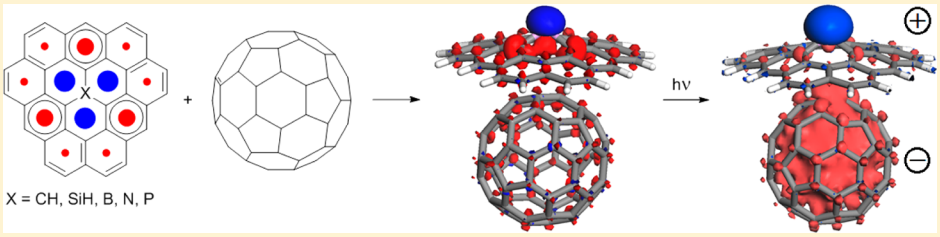

ABSTRACT: Density functional theory (DFT) and semiempirical UHF natural orbital configuration interaction (UNO-CI) calculations are used to investigate the effect of heteroatom substitution at the central position of a model polycyclic aromatic hydrocarbon. The effects of the substitution on structure, strain, electronic and spectral properties, and aromaticity of the compounds are discussed.

INTRODUCTION

Polycyclic aromatic hydrocarbons (PAHs)[1] exhibit extended two-dimensional (2D) π-conjugation, which makes them particularly interesting for use in organic electronic devices (e.g., organic light-emitting diodes (OLEDs), field effect transistors (OFETs), and photovoltaic cells) as they can provide pathways for charge transport through columnar arrays.[2,3] PAHs have also won increased interest because of the current developments in the field of new carbon allotropes,[4] where extended planar and nonplanar polyaromatic systems represent defined molecular fragments of graphene, fullerenes and carbon nanotubes and have hence become attractive objects for experimental and theoretical studies.[5−9]

The technically important optoelectronic (e.g., band gaps) and self-assembly properties of PAHs can be tuned by modifying the size and periphery of the π-conjugated system or/and by lateral decoration with suitable substituents.[10,11] However, the most efficient strategy for tuning the properties of PAHs is to incorporate heteroatoms directly into their sp^2-carbon skeletons.[12] Thus, without dramatic structural modifications of the polycyclic scaffold, either vacancies (holes) or low-lying nonbonding states (electrons) can be introduced upon insertion of electron-deficient and electron-rich heteroatoms, respectively. In most cases, the heteroatoms, such as boron, nitrogen, phosphorus, oxygen, and sulfur, are located at the periphery of the π systems, which improves their synthetic accessibility.[13−21] This approach has led to many interesting systems with appealing optoelectronic properties, whose performance in devices has been studied.[17,20] Compounds containing Lewis basic heteroatoms at geometrically favorable positions at the periphery have been shown to form supramolecular architectures upon coordination to transition-metal centers.[16,18] In contrast, reports of fascinating but synthetically much more challenging π-conjugated frameworks with interior or ring-junction heteroatoms remain scarce.[22−29] Only recently, Yamaguchi and co-workers prepared several planar triarylboranes that are highly stable toward water and oxygen because of the unique structural constraints on the central boron atom.[26,29] The limited number of similar compounds with central heteroatoms is all the more surprising as numerous theoretical investigations have suggested that such systems can act as defined molecular substructures of heteroatom-doped nanocarbons.[30−41] Such selectively doped PAHs represent intriguing research targets as the efficient electronic interaction between the heteroatom and the π-system should result in both strongly altered photophysical and redox properties and π-stacking behavior when compared to their all-carbon counterparts.[22−35]

Stimulated by previous theoretical studies of the π-stacking behavior of nitrogen-containing PAHs,[35] we designed a series of π-conjugated scaffolds **1**−**5** that contain central CH, SiH, B, N, and P moieties. The synthesis of these molecules is currently being pursued in our laboratory. Depending on the nature of the central heteroatom, we expect these systems to act as directional charge conductors when arranged into extended

Special Issue: Howard Zimmerman Memorial Issue

Received: August 30, 2012
Published: October 22, 2012

Chart 1. Systems 1−5 Studied in This Work

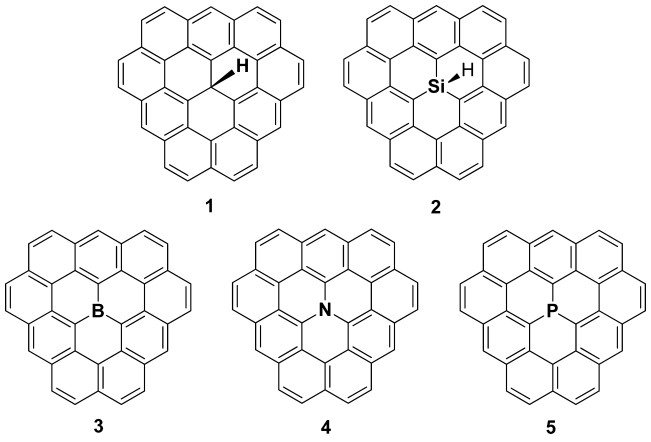

columnar assemblies or to form charge-transfer complexes with suitable partners to give attractive photophysical properties. Here, we have used extensive quantum chemical calculations to determine a variety of physicochemical properties of **1**−**5**. The results provide useful guidelines for designing advanced functional materials for use in devices.

COMPUTATIONAL DETAILS

All density-functional theory (DFT) calculations were performed with the Gaussian 09 program suite[42] and all semiempirical computations with Vamp 11.0.[43] We have calculated normal vibrational modes within the harmonic approximation to characterize both minima and transition states (TS).[44] Zero-point energy (ZPE) corrections calculated at ωB97XD[45]/6-31G(d)[46−57] were added to the Born−Oppenheimer energies calculated at DFT. No symmetry constraints were applied during optimizations.

RESULTS AND DISCUSSION

Geometry, Spin State, and Relative Stability. Since we are interested in electron-transfer processes between **1**−**5** and donors and acceptors (vide infra), we have chosen the ωB97XD/6-31G(d) level of theory to optimize all molecules because the ωB97XD functional includes long-range dispersion corrections[45] that are necessary to describe geometries of the donor−acceptor dyads with a strong π−π interactions properly[58] and because we have found this level of theory to be reliable.[59]

The ground states of molecules **1**−**5** are found to be singlets and the lowest lying triplet states more than 1.6 eV higher in energy at ωB97XD/6-31G(d). The smallest singlet−triplet gap is found for phosphorus-doped **5** followed by **1** and the largest for the boron- and nitrogen-containing compounds **3** and **4** (Table 1).

However, large PAHs are known to have singlet ground states with significant open-shell singlet character.[60] This can be quantified using the diradical character *y*, which indicates the contribution of the singlet diradical to the ground state.[60,61] The diradical character can be estimated from the occupation numbers of the frontier unrestricted (HF) natural orbitals (UNOs) using a simple eq 1[61]

$$y = 100\% - \frac{4(\sigma_{HOMO} - \sigma_{LUMO})}{4 + (\sigma_{HOMO} - \sigma_{LUMO})^2}100\% \quad (1)$$

where σ_{HOMO} and σ_{LUMO} are the occupation numbers of highest occupied and lowest unoccupied molecular orbitals, respectively. We have shown previously that *y* values obtained using occupations of semiempirical (PM6[62]) UNOs agree well with experimental estimates[63] so that this level of theory was used to calculate the diradical characters of **1**−**5**.

Table 1. Energy Differences between Triplet and Singlet Spin States of 1−5 ($\Delta E_{triplet-singlet}$, eV) and Inclusion Energies ($\Delta E_{inclusion}$, kcal mol^{-1}) of Species 1−5 According to the Isodesmic Equation Shown in Scheme 1 at the ωB97XD/6-31G(d) level; Occupation Numbers (σ) of Frontier UHF Natural Orbitals (UNOs) and Diradical Characters (*y*) of 1−5 at PM6[a]

species	$\Delta E_{triplet-singlet}$	σ_{HOMO}	σ_{LUMO}	*y* (%)	$\Delta E_{inclusion}$
1	1.77	1.598	0.402	12	43.8
2	2.22	1.619	0.381	10	77.2
3	2.50	1.628	0.372	10	35.0
4	2.44	1.615	0.385	11	27.1
5	1.60	1.591	0.409	12	61.5

[a]The DIIS[64] SCF-convergence technique was used for **1**−**5**. AM1[65−69] density matrices were used as initial guesses for **1**, **3**, and **4** and AM1*[70,71] for **2** and **5**.

Despite their relatively large singlet−triplet gaps, the compounds studied have significant diradical characters of approximately 10% for all species (Table 1), with the largest values for **1** and **5**. This suggests that **1**−**5** are promising candidates for nanosized electronic devices[60] but also that they are reactive.

The calculations suggest that molecules **1** and **2** are bowl-shaped (Figure 1) because of the sp^3-hybridized central carbon and silicon atoms. **2** is more curved than **1** ($\angle C_{sp^2}SiC_{sp^2}$ = 103.1° compared with $\angle C_{sp^2}C_{sp^3}C_{sp^2}$ = 114.2°; see Figure S1 of the Supporting Information) because of the longer Si−C_{sp^2} bonds (1.805 Å) compared with C_{sp^3}−C_{sp^2} (1.505 Å, Figure S1, Supporting Information). Compounds **3** and **4** are planar, while **5** is bowl-shaped ($\angle C_{sp^2}PC_{sp^2}$ = 99.4°, Figure S1, Supporting Information) because of the long P−C_{sp^2} bonds and small inherent bond angles at phosphorus. The inversion barrier of **5** via the planar transition state **TS1** (Figure 1) is 37.0 kcal mol^{-1} at ωB97XD/6-31G(d).

We have used the isodesmic equation shown in Scheme 1 to calculate inclusion energies of **1**−**5**.

All inclusion energies are endothermic (Table 1) because of the strain introduced into the polycyclic skeleton. The least endothermic is the inclusion of nitrogen and the most endothermic silicon, indicating that **2** is the most deformed and strained of the molecules **1**−**5**.

Electronic Structure. To assess the donor-accepting properties of the species **1**−**5**, we have calculated their ability to attach and detach an electron at the OLYP[73−76]/6-311+G(d,p)[47−50,53−57,77−79] level of theory on the ωB97XD/6-31G(d)-optimized geometries. Physicochemical properties calculated with OLYP/6-311+G(d,p) are in good agreement with experiment for a range of organic semiconductors.[80,81] On the other hand, large basis sets that include diffuse functions are necessary to describe anions properly.[77]

As expected, nitrogen behaves as an *n*-dopant of PAH, and thus, **4** has the lowest electron affinity (EA) and ionization potential (IP) (Table 2). On the other hand, boron is a *p*-dopant, and therefore, **3** has the largest EA and IP values. N-doping has a much larger effect on EA than on IP and vice versa for *p*-doping. Interestingly, **1** and **5** have very close values of EA and IP because both the CH-moiety and the phosphorus atom

dx.doi.org/10.1021/jo3018395 | J. Org. Chem. 2013, 78, 1894−1902

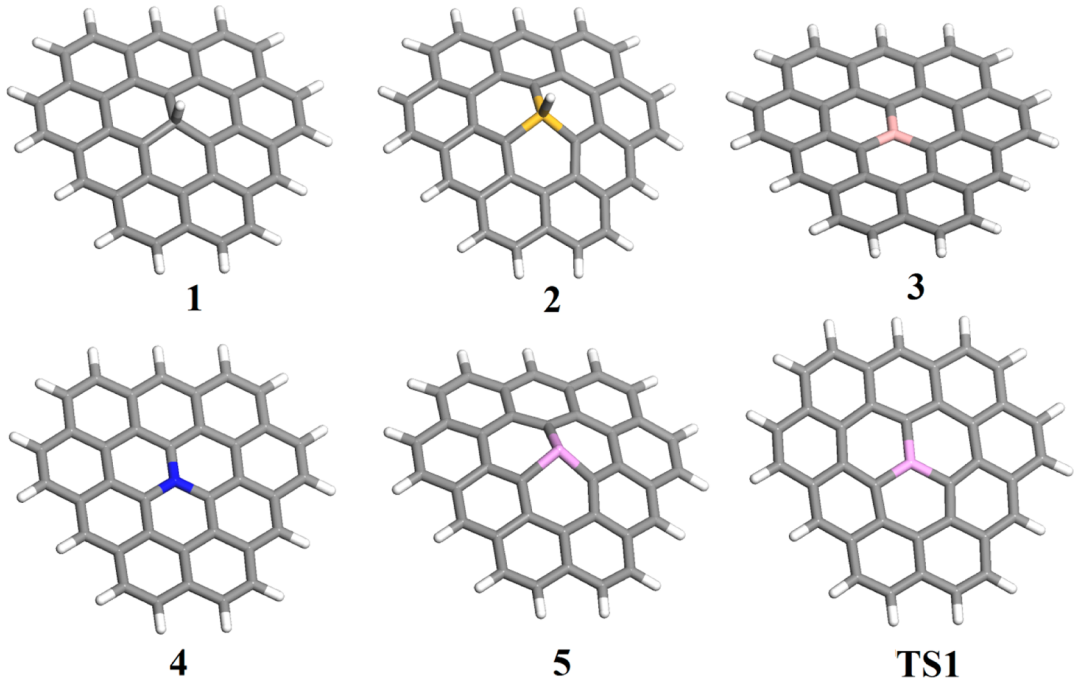

Figure 1. Geometries of **1**−**5** and **TS1** visualized with Materials Studio 6.0.[72]

Scheme 1. Isodesmic Equation Used To Calculate Inclusion Energies of 1−5[a]

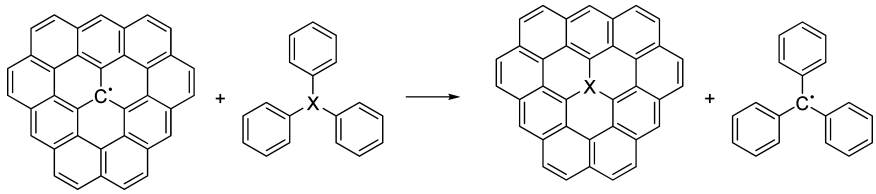

[a]X = CH (**1**), SiH (**2**), B (**3**), N (**4**), and P(**5**).

Table 2. Vertical and Adiabatic Electron Affinities (EA_v and EA_a) and Ionization Potentials (IP_v and IP_a) and Transport Band Gaps (E_t) of 1−5 in eV at OLYP/6-311+G(d,p)

species	IP_v	EA_v	IP_a	EA_a	E_t
1	5.86	1.40	5.77	1.54	4.23
2	6.08	1.66	6.14	1.80	4.34
3	6.81	1.95	6.89	2.05	4.84
4	5.39	0.64	5.36	0.65	4.71
5	5.86	1.49	5.75	1.62	4.13

conjugate with the π-framework of the PAH weakly. Moreover, CH and P do not deform the PAH skeleton as strongly as the SiH-moiety, which deforms the skeleton significantly leading to higher EA and IP values of **2** relative to **1** and **5**.

We have calculated transport band gaps (E_t) of **1**−**5** as defined in eq 2:

$$E_t = IP_a - EA_a \quad (2)$$

The lowest transport band gaps are for **1**, **2**, and **5**, while the largest are for **3** and **4** because of the much stronger influence of N- and B-doping on donor and acceptor abilities observed above, while HOMO and LUMO levels are not as strongly affected by CH, SiH and P doping (see also Figure 2).

Optical (absorption) band gaps E_{opt} were calculated at the MNDO UNO-CIS[63] level of theory because semiempirical UNO-CI methods predict quite accurate E_{opt} for different organic molecules[63] including heterocycles.[80] The values obtained were compared with optical band gaps calculated at the TD[82−90] B3LYP[73,74,91]/6-311++G(d,p)[47−50,53−57,77−79] level of theory. E_{opt} is equal to the energy of the lowest lying excited state with significant oscillator strength and in experiments is identified as the lowest energy peak in the UV−vis absorption spectrum. On the other hand, the lowest excitation energies correspond to electronic band gaps of the molecules.

Both methods predict that **1** has the largest optical band gap, closely followed by **5** (Table 3), while the lowest E_{opt} is found for N-doped **4**, while B-doped **3** has a somewhat larger band gap. The band gap of **2** calculated at MNDO UNO-CIS is lower than E_{opt} of **3**, in disagreement with the order predicted by TDDFT, although the absolute difference between optical band gaps of **2** and **3** is quite small (0.17−0.28 eV) and falls in the range of accuracy of both the semiempirical CIS and TDDFT methods. Molecular electronic band gaps E_{elec} are found to be 1.00 ± 0.15 eV for all species at MNDO UNO−CIS and 1.50 ± 0.25 eV with TDDFT.

The optical transition that corresponds to the optical band gap arises from the formation of the Frenkel exciton.[92] Frenkel exciton represents the electron and hole located on the molecule of the doped PAH. The interaction between the electron and hole assessed by exciton binding energy (BE_{ex}) is very important property for the nanoelectronics devices based

dx.doi.org/10.1021/jo3018395 | J. Org. Chem. 2013, 78, 1894−1902

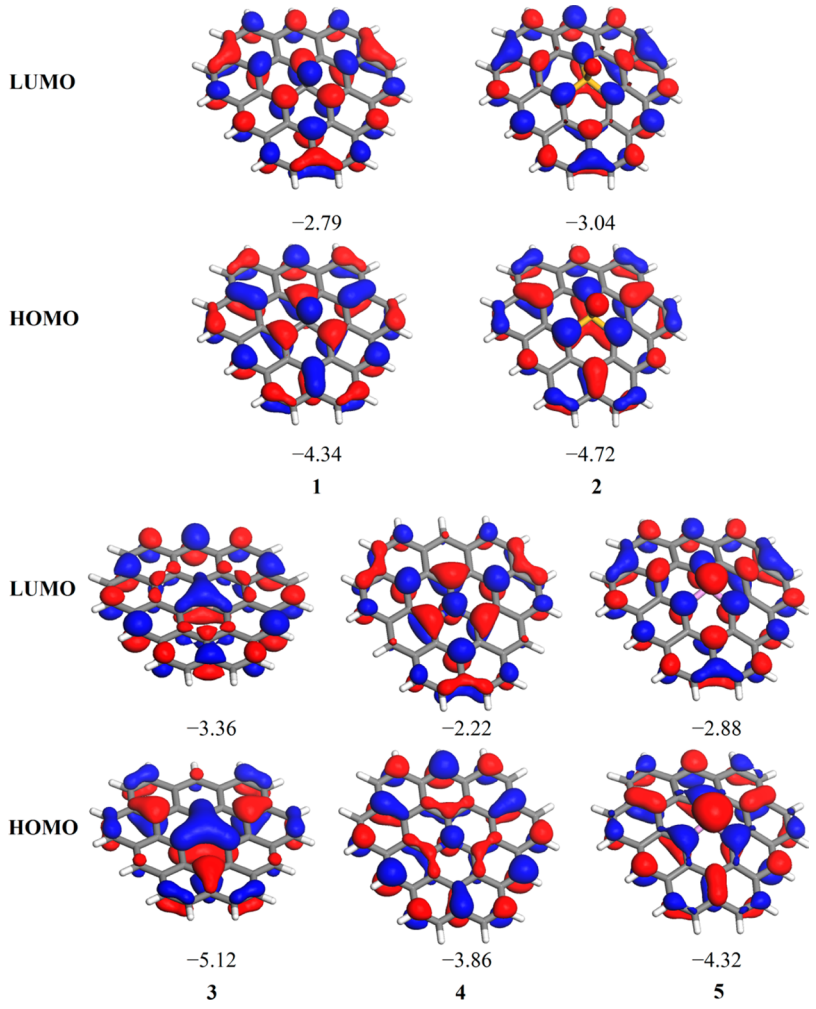

Figure 2. Frontier molecular orbitals of **1**−**5** visualized with Materials Studio 6.0.[72] HOMO and LUMO energies in eV at OLYP/6-311+G(d,p)//ωB97XD/6-31G(d).

Table 3. Optical (E_{opt})[a] and Electronic Band Gaps (E_{elec}) in eV at MNDO UNO-CIS[b] and TD B3LYP/6-311++G(d,p) (Exciton Binding Energies (BE_{ex}) in eV)

	MNDO UNO-CIS				TD B3LYP/6-311++G(d,p)			
species	E_{opt}	f	E_{elec}	BE_{ex}	E_{opt}	f	E_{elec}	BE_{ex}
1	2.84	0.095	1.05	1.39	3.16	0.124	1.36	1.07
2	2.56	0.011	1.06	1.78	2.78	0.080	1.52	1.56
3	2.73	0.147	1.14	2.11	2.50	0.163	1.71	2.34
4	2.42	0.139	0.96	2.29	2.42	0.122	1.58	2.29
5	2.84	0.078	1.05	1.29	3.01	0.092	1.25	1.12

[a]Excitations with oscillator strength below 0.01 are usually too weak to be observed experimentally and were therefore ignored. [b]The number of orbitals in the active space was 36 for all species.

on organic semiconductors. It can be defined as the difference between transport and optical band gaps:[92−95]

$$BE_{ex} = E_t - E_{opt} \quad (3)$$

Excitons are the most strongly bound in **3** and **4** (2.11−2.34 eV) and the most weakly in **1** and **5** (1.07−1.39 eV), while the BE_{ex} value for **2** (1.56−1.78 eV) lies in between (Table 3). All values are typical for excitons located within a molecule of middle-sized PAH like pentacene.[94,96] The reason for this trend maybe lesser spatial distribution of the exciton wave function and decreased dielectric screening[97] in **3** and **4** in comparison with that of **1**, **2**, and **5**. On the other hand, the stronger deformation induced by SiH moiety than by CH and P leads to larger BE_{ex} value in **2** than in **1** and **5**.

Photoinduced Electron Transport. Photoinduced electron transport (PIET) depends strongly on the distance between donor and acceptor. For instance, PIET was observed as a charge-transfer band in the UV−vis absorption spectra for porphyrin−fullerene dyads in which the electroactive moieties are close to each other.[58] The distance between them (ca. 3 Å) is similar to that found in cocrystals of C_{60} and H_2TPP.[58] In addition, cocrystals of fullerene with aromatic amines undergo PIET.[98]

dx.doi.org/10.1021/jo3018395 | J. Org. Chem. 2013, 78, 1894−1902

Table 4. Binding Energies of 1−5 with Fullerene and Porphin H_2P and in $H_2P{\cdot}C_{60}$ in kcal mol^{-1} at ωB97XD/6-31G(d)[a,b]

					gas		toluene	
species	binding energy	RMSD[c]	R_{min}	$R_{E\text{-complex}}$	Q_{GS}[d]	D_{GS}	Q_{GS}[d]	D_{GS}
$\mathbf{1}{\cdot}C_{60}$	−24.4	0.094	3.059	3.307	0.00	0.1	0.00	0.1
$\mathbf{2}{\cdot}C_{60}$	−30.2	0.070	3.199	3.787	0.00	0.0	0.00	0.1
$\mathbf{3}{\cdot}C_{60}$	−22.4	0.217	2.979		0.00	0.6	0.00	0.7
$\mathbf{4}{\cdot}C_{60}$	−21.1	0.088	2.898		0.00	0.0	0.00	0.1
$\mathbf{5}{\cdot}C_{60}$	−28.0	0.074	3.169	3.828	0.00	1.9	0.00	2.2
$\mathbf{1}{\cdot}H_2P$	−32.5	0.052	3.227	3.966	0.00	0.1	0.00	0.1
$\mathbf{2}{\cdot}H_2P$	−29.2	0.059	3.074	4.753	0.00	0.3	0.00	0.4
$\mathbf{3}{\cdot}H_2P$	−33.4	0.034	3.309	3.472	0.00	0.2	0.00	0.3
$\mathbf{4}{\cdot}H_2P$	−34.3	0.075	3.327	3.524	0.00	0.1	0.00	0.2
$\mathbf{5}{\cdot}H_2P$	−31.1	0.066	3.132	4.629	0.00	1.9	0.00	2.2
$H_2P{\cdot}C_{60}$	−21.2	0.100	2.781		0.00	0.2	0.00	0.2

[a]Root mean square deviations (RMSD) in Å of **1**−**5** and H_2P structures in complexes with C_{60} or H_2P relative to free **1**−**5** and H_2P. The minimal (R_{min}) interatomic distances between **1**−**5** or H_2P and C_{60} or H_2P and the closest distances between the central atom E = C, Si, B, N, P of **1**−**5** and any atom of C_{60} or H_2P ($R_{E\text{-complex}}$) in Å. Values of charge transfer (Q_{GS}) equal to charge on **1**−**5** or H_2P moieties in their complexes with C_{60} or H_2P in *e* and dipole moments (D_{GS}) in debye in the ground states (GS) from MNDO UNO-CIS calculations in the gas phase and toluene. [b]Densities from the gas-phase calculations were taken as initial guesses for calculations in toluene. [c]Calculated with Chemcraft 1.6.[99] [d]Calculated by summing the Coulson charges from the UNO−CI calculations.

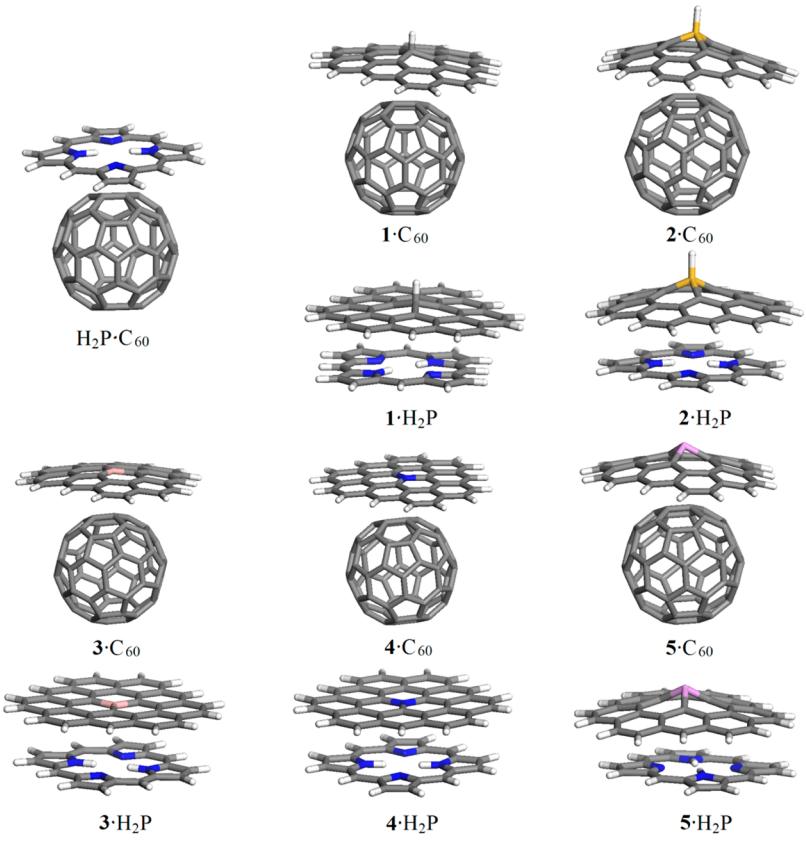

Figure 3. Complexes (**1**−**5**)·C_{60}, (**1**−**5**)·H_2P, and $H_2P{\cdot}C_{60}$ calculated at the ωB97XD/6-31G(d) level.

We have therefore calculated the complexation energies of compounds **1**−**5** with C_{60} and porphyrin H_2P (as a model for H_2TPP) and compared them to the binding energies of C_{60} to H_2P at the ωB97XD/6-31G(d) level of theory. The complexation energies of PAHs **1**−**5** to C_{60} and H_2P are generally stronger that those of H_2P to C_{60} (Table 4). Compounds **2** and **5**, and to a lesser degree **1** ,have the largest binding energies to fullerene because their bowl-shaped form matches the ball shape of C_{60} much better than planar **3** and **4** (Figure 3).

Interaction with fullerene deforms the complexed molecules. This RMSD deformation is in the range of 0.1 Å (Table 4) except for the complex between **3** and C_{60}, in which the electron-accepting fullerene pulls the boron atom out of the plane. The nitrogen atom in **4** binds most strongly to C_{60}, leading to the closest intermolecular distances between PAH and C_{60} (compare interatomic distances between central atom of PAH and carbon atom of C_{60} and the minimal interatomic distances between PAHs, H_2P and C_{60}, Table 4). On the other hand, planar **3** and **4** are more strongly bound to the planar

dx.doi.org/10.1021/jo3018395 | J. Org. Chem. 2013, 78, 1894−1902

Table 5. Energies of the Lowest Lying CT States above Ground States of the Complexes 1−5 with C_{60} and H_2P (E_{CT}) in eV, Oscillator Strengths (f) of Respective Transitions at MNDO UNO-CIS[a,b]

	gas				toluene			
specie	E_{CT}	f	Q_{CT}	D_{CT}	E_{CT}	f	Q_{CT}	D_{CT}
1·C_{60}	3.09	2.28×10^{-3}	0.85	18.0	2.95	6.45×10^{-4}	0.98	24.6
2·C_{60}	3.18	1.39×10^{-3}	0.70	13.6	3.06	1.44×10^{-3}	0.72	14.0
3·C_{60}	3.63	8.24×10^{-3}	0.87	18.0	3.41	4.40×10^{-3}	0.89	18.3
4·C_{60}	2.45	4.03×10^{-3}	0.97	21.7	2.19	2.09×10^{-3}	0.98	21.9
5·C_{60}	3.14	6.36×10^{-4}	0.91	16.7	2.99	7.96×10^{-4}	0.84	14.9
1·H_2P	3.06	1.78×10^{-4}	−0.65	10.7	3.06	1.59×10^{-4}	−0.20	3.3
	3.06	5.31×10^{-5}	0.66	10.9	3.04	5.72×10^{-5}	0.21	3.4
	3.22	1.38×10^{-3}	−0.98	16.1	3.00	1.38×10^{-3}	0.98	16.2
	3.32	3.41×10^{-4}	0.98	16.1	3.18	3.52×10^{-4}	−0.98	16.1
2·H_2P	3.11	9.52×10^{-5}	−0.98	16.9	2.96	9.51×10^{-5}	−0.98	16.9
3·H_2P	2.53	1.35×10^{-3}	−0.78	12.4	2.44	1.37×10^{-3}	−0.78	12.4
4·H_2P	2.30	4.21×10^{-4}	0.93	15.1	2.11	4.34×10^{-4}	0.92	15.0
5·H_2P	3.12	5.12×10^{-5}	−0.98	18.4	2.93	6.46×10^{-5}	−0.98	18.6
H_2P·C_{60}	2.56	1.30×10^{-3}	0.98	20.2	2.30	1.28×10^{-3}	0.99	20.3

[a]Values of charge transfer (Q_{GS}) equal to charge on **1**−**5** or H_2P moieties in their complexes with C_{60} or H_2P in e and dipole moments (D_{GS}) in debye in charge-transfer states from MNDO UNO-CIS calculations in the gas phase and toluene. [b]Densities from the gas-phase calculations were taken as initial guesses for calculations in toluene.

porphyrin than the bowl-shaped PAHs. Note that the ground-state complexes do not exhibit significant intermolecular charge transfer (CT); the values of charge transfer determined from population analyses are essentially zero and the dipole moments of the complexes are very small (Table 4).

Finally, we have calculated the excitations that lead to charge-separated states in the complexes of **1**−**5** with C_{60} as acceptor and with H_2P using the MNDO UNO-CIS method[63] on the ωB97XD/6-31G(d)-optimized geometries because the semiempirical UNO-CIS approach has been used successfully to reveal the nature of the charge-transfer states of porphyrin−fullerene dyads.[58]

C_{60} behaves as the acceptor in all singlet CT states observed for complexes of **1**−**5** with fullerene. The amount of charge transferred is always larger than 0.70 e and the dipole moments larger than 10 D (Table 5). Since **4** is the strongest donor, the absorption charge transfer band is located at the lowest energy (2.45 eV, even lower than in H_2P·C_{60}) and the charge transferred from **4** to C_{60} is largest (0.97 e). In contrast, **3** is the weakest donor among **1**−**5** and therefore the energy of CT state is highest (3.63 eV), although amount of charge transferred in **3**·C_{60} is larger than in **2**·C_{60} because the intermolecular distance in **3**·C_{60} is smaller than in **2**·C_{60}. Oscillator strengths of the ground state (GS) to CT state transitions are calculated to be ca. 1×10^{-3}, indicating that weak CT absorption bands are observable in UV−vis spectra.[58] Note that semiempirical UNO-CIS usually overestimates the energy of CT states;[58] thus, these values may lie about 0.5 eV lower than found in the calculations. Porphyrin H_2P behaves as a donor in the complex with fullerene and with **1**−**3** and **5** in the gas phase. However, the strong donor as **4** donates an electron to H_2P in the CT complex.

Solvation effects taken into account using the polarizable continuum model self-consistent reaction field (PCM-SCRF) technique[100] can shift the absorption charge transfer bands to the longer wavelength region substantially, even for such a weakly polar solvent as toluene (Table 5). Moreover, solvation can stabilize some excited states more than others, thus changing their order and in the case of **1**·H_2P even the direction of charge transfer: in the gas phase, an electron is transferred from the porphyrin to **1** and in toluene from **1** to the porphyrin (Table 5).

Thus, we can expect that complexes of **1**−**5** with different acceptors and donors can undergo photoinduced electron transport, the direction of which depends on the relative donor−acceptor properties of complexes and solvent effects.

Aromaticity. Nucleus-independent chemical shifts[101−103] (NICSs) values at the centers of rings **A**, **B**, **C** of **1**−**5** (Chart 2), i.e., NICSs(0) values, were calculated with the gauge-independent atomic orbital (GIAO) method[104−109] at the B3LYP/6-311+G(d,p) level of theory on ωB97XD/6-31G(d)-optimized geometries. The results are summarized in Table 5.

Chart 2. Numbering of Rings of 1−5, Where X = CH (1), SiH (2), B (3), N (4), and P(5)[a]

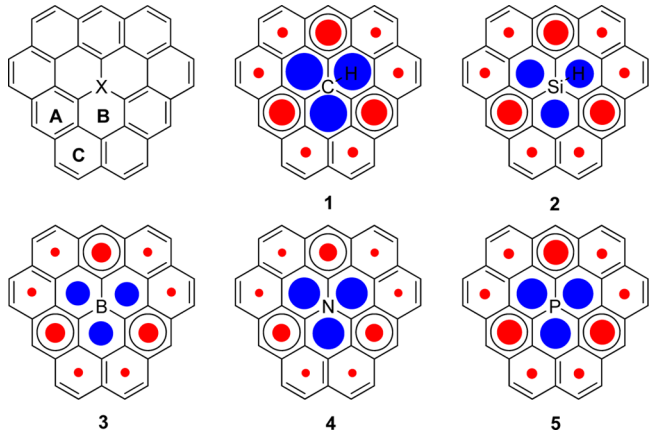

[a]Denoting three rings **A**−**C** is sufficient to define each ring because of the D_{3h} symmetry of the molecules. Representation of aromaticity of **1**−**5** with Clar's sextets; the size of the solid dots inside rings represents the relative aromaticity (red) and antiaromaticity (blue) of the rings.

The **A** rings are aromatic as their NICS values are significantly negative, while the **C** rings are essentially nonaromatic and the **B** rings are antiaromatic. Thus, the

dx.doi.org/10.1021/jo3018395 | J. Org. Chem. 2013, 78, 1894−1902

aromaticity of **1**−**5** can be described by Clar's sextets[110−112] (Chart 2), in which the π-electrons of the **A** rings are in sextet rings and those of **C** rings are assigned to double bonds. The central moiety is not part of the aromatic system but can influence aromaticity of the neighboring aromatic framework by introducing geometrical deformations (**1**, **2**, and **5**), the mesomeric effect (**3**, **4**, and to a lesser degree **5**) and the inductive effect (**1**−**5**). The strongest factor is the mesomeric effect. As we have seen above, the lone pair of nitrogen and the vacant orbital of boron interact with the π-system most strongly leading to the most significant lowering of aromaticity in **3** and **4** relative to **1**, **2**, and **5** (Table 6). Much larger structural deformation in **2** and **5** than in **1** leads to somewhat less negative NICS values at the centers of the **A** rings, while the more distant **C** rings are less affected.

Table 6. NICSs(0) Values at the Centers of Rings A−C of 1−5 Calculated at the SCF-GIAO B3LYP/6-311+G(d,p) Level of Theory on the ωB97XD/6-31G(d)-Optimized Geometries

	ring		
species	A	B	C
1	−8.8	12.5	−3.5
2	−8.4	9.5	−3.5
3	−6.6	8.1	−3.0
4	−6.0	10.6	−2.7
5	−8.4	10.3	−3.5

CONCLUSIONS

Both density functional theory (DFT) and semiempirical unrestricted natural orbital−configuration interaction (UNO−CI) calculations have revealed three distinct groups of doped PAHs with central CH, SiH groups and N, B, or P heteroatoms: (1) CH- and P-doped PAHs, in which the heteroatom does not interact significantly with the π-system, (2) SiH-doped PAH, whose planar PAH skeleton is very strongly deformed, leading to significant changes in electronic properties, (3) B- and N-doped PAHs, in which the heteroatoms interact strongly with the π-system of the remainder of the molecule in opposite directions. All systems studied have significant singlet diradical character, making them attractive for use in nanoelectronics devices. Moreover, they are all semiconductors with the largest optical band gaps for the group 1 compounds, **1** and **5** and with the lowest band gap for N-doped PAH **4**. Because the electronic communication between the central group and the remaining π-system is most effective in group 3 compounds, molecules **3** and **4** represent the upper and lower ends of the electrochemical behavior range of compounds **1**−**5**; **3** has the largest and **4** the smallest EA and IP values. In addition, these compounds can be used as electron donors and acceptors in stable complexes with such compounds as fullerenes or porphyrins under photo-irradiation. The direction of electron transport can be controlled not only by changing the electron donors and acceptor molecules, but also by different solvents. The calculated NICSs values of compounds **1**−**5** at the centers of their rings revealed that the central rings are antiaromatic and that rings of the next layer are aromatic, whereas the peripheral ones have olefinic character and are thus probably available for addition reactions. The results obtained for the above compounds can be used to understand the electronic properties of doped graphenes better, which will in turn allow targeted manipulation of electronic properties of graphene by doping.

ASSOCIATED CONTENT

Supporting Information

Total energies, zero-point energies, numbers of imaginary frequencies, and *XYZ* coordinates of all calculated species at the ωB97XD/6-31G(d) and total energies of **1**−**5** and their ions at OLYP/6-311+G(d,p)//ωB97XD/6-31G(d). Visualized geometries of **1**−**5** species with all bond lengths and selected bond angles. This material is available free of charge via the Internet at http://pubs.acs.org.

AUTHOR INFORMATION

Corresponding Author

*E-mail: (T.C.) tim.clark@chemie.uni-erlangen.de, (M.K.) milan.kivala@chemie.uni-erlangen.de.

Notes

The authors declare no competing financial interest.

ACKNOWLEDGMENTS

This work was supported by the Deutsche Forschungsgemeinschaft (DFG) as part of SFB953 "Synthetic Carbon Allotropes" and by the "Solar Technologies Go Hybrid" initiative of the State of Bavaria. We also thank the Regional Computing Center Erlangen (RRZE) and the Leibniz Rechenzentrum Munich for computational resources. P.O.D. thanks the Graduate School Molecular Science and Universität Bayern e.V. for a stipend within the Bavarian Elite Aid Program.

DEDICATION

In memory of Howard Zimmerman.

REFERENCES

(1) Clar, E. *Polycyclic Hydrocarbons*; Academic Press: New York, 1964; Vol. *I/II*.
(2) Pisula, W.; Feng, X.; Müllen, K. *Chem. Mater.* **2011**, *23*, 554.
(3) Wu, J. S.; Pisula, W.; Müllen, K. *Chem. Rev.* **2007**, *107*, 718.
(4) Hirsch, A. *Nat. Mater.* **2010**, *9*, 868.
(5) Petrukhina, M. A., Scott, L. T., Eds.; John Wiley & Sons, Inc.: New York, 2012.
(6) Chen, L.; Hernandez, Y.; Feng, X.; Müllen, K. *Angew. Chem., Int. Ed.* **2012**, *51*, 7640−7654.
(7) Dias, J. R. *J. Phys. Chem. A* **2008**, *112*, 12281.
(8) Feng, C.; Lin, C. S.; Fan, W.; Zhang, R. Q.; Van Hove, M. A. *J. Chem. Phys.* **2009**, *131*, 194702/1.
(9) Mishra, P. C.; Yadav, A. *Chem. Phys.* **2012**, *402*, 56.
(10) Feng, X.; Marcon, V.; Pisula, W.; Hansen, M. R.; Kirkpatrick, J.; Grozema, F.; Andrienko, D.; Kremer, K.; Müllen, K. *Nat. Mater.* **2009**, *8*, 421.
(11) Rieger, R.; Müllen, K. *J. Phys. Org. Chem.* **2010**, *23*, 315.
(12) Kervyn, S.; Aurisicchio, C.; Bonifazi, D. In *Functional Supramolecular Architectures*; Samorì, P., Cacialli, F., Eds.; Wiley-VCH: Weinheim, 2011; p 233.
(13) For recent examples of PAHs with peripheral heteroatoms, see refs 14−21.
(14) Agou, T.; Kobayashi, J.; Kawashima, T. *Chem. Commun.* **2007**, 3204.
(15) Bouit, P.-A.; Escande, A.; Szűcs, R.; Szieberth, D.; Lescop, C.; Nyulászi, L.; Hissler, M.; Réau, R. *J. Am. Chem. Soc.* **2012**, *134*, 6524.
(16) Draper, S. M.; Gregg, D. J.; Madathil, R. *J. Am. Chem. Soc.* **2002**, *124*, 3486.
(17) Gorodetsky, A. A.; Chiu, C. Y.; Schiros, T.; Palma, M.; Cox, M.; Jia, Z.; Sattler, W.; Kymissis, I.; Steigerwald, M.; Nuckolls, C. *Angew. Chem., Int. Ed.* **2010**, *49*, 7909.

(18) Gregg, D. J.; Fitchett, C. M.; Draper, S. M. *Chem. Commun.* **2006**, 3090.
(19) Jiang, W.; Qian, H. L.; Li, Y.; Wang, Z. *J. Org. Chem.* **2008**, *73*, 7369.
(20) Wei, J.; Han, B.; Guo, Q.; Shi, X.; Wang, W.; Wei, N. *Angew. Chem., Int. Ed.* **2010**, *49*, 8209.
(21) Wu, D. Q.; Pisula, W.; Haberecht, M. C.; Feng, X.; Müllen, K. *Org. Lett.* **2009**, *11*, 5686.
(22) For recent examples of PAHs with interior or ring-junction heteroatoms, see refs 23−29.
(23) Bosdet, M. J. D.; Piers, W. E.; Sorensen, T. S.; Parvez, M. *Angew. Chem., Int. Ed.* **2007**, *46*, 4940.
(24) Hatakeyama, T.; Hashimoto, S.; Nakamura, M. *Org. Lett.* **2011**, *13*, 2130.
(25) Hatakeyama, T.; Hashimoto, S.; Seki, S.; Nakamura, M. *J. Am. Chem. Soc.* **2011**, *133*, 18614.
(26) Saito, S.; Matsuo, K.; Yamaguchi, S. *J. Am. Chem. Soc.* **2012**, *134*, 9130.
(27) Takase, M.; Enkelmann, V.; Sebastiani, D.; Baumgarten, M.; Müllen, K. *Angew. Chem., Int. Ed.* **2007**, *46*, 5524.
(28) Wu, D.; Liu, R.; Pisula, W.; Feng, X.; Müllen, K. *Angew. Chem., Int. Ed.* **2011**, *50*, 2791.
(29) Zhou, Z.; Wakamiya, A.; Kushida, T.; Yamaguchi, S. *J. Am. Chem. Soc.* **2012**, *134*, 4529.
(30) Álvarez-Collado, J. R. *Theor. Chem. Acc.* **2011**, *128*, 223.
(31) Hasegawa, T.; Suzuki, T.; Mukai, S. R.; Tamon, H. *Carbon* **2004**, *42*, 2195.
(32) Khavryuchenko, V. D.; Khavryuchenko, O. V.; Tarasenko, Y. A.; Lisnyak, V. V. *Chem. Phys.* **2008**, *352*, 231.
(33) Kurita, N.; Endo, M. *Carbon* **2002**, *40*, 253.
(34) Mandumpal, J.; Gemming, S.; Seifert, G. *Chem. Phys. Lett.* **2007**, *447*, 115.
(35) Tran, F.; Alameddine, B.; Jenny, T. A.; Wesolowski, T. A. *J. Phys. Chem. A* **2004**, *108*, 9155.
(36) For recent examples of PAHs with interior or ring-junction heteroatoms, see refs 37−41.
(37) Kawaguchi, M. *Adv. Mater.* **1997**, *9*, 615.
(38) Liu, H.; Liu, Y.; Zhu, D. *J. Mater. Chem.* **2011**, *21*, 3335.
(39) Lv, R. T.; Terrones, M. *Mater. Lett.* **2012**, *78*, 209.
(40) Vostrowsky, O.; Hirsch, A. *Chem. Rev.* **2006**, *106*, 5191.
(41) Terrones, M.; Jorio, A.; Endo, M.; Rao, A. M.; Kim, Y. A.; Hayashi, T.; Terrones, H.; Charlier, J.-C.; Dresselhaus, G.; Dresselhaus, M. S. *Mater. Today* **2004**, *7*, 30.
(42) Frisch, M. J.; Trucks, G. W.; Schlegel, H. B.; Scuseria, G. E.; Robb, M. A.; Cheeseman, J. R.; Scalmani, G.; Barone, V.; Mennucci, B.; Petersson, G. A.; Nakatsuji, H.; Caricato, M.; Li, X.; Hratchian, H. P.; Izmaylov, A. F.; Bloino, J.; Zheng, G.; Sonnenberg, J. L.; Hada, M.; Ehara, M.; Toyota, K.; Fukuda, R.; Hasegawa, J.; Ishida, M.; Nakajima, T.; Honda, Y.; Kitao, O.; Nakai, H.; Vreven, T.; Montgomery, J. A., Jr.; Peralta, J. E.; Ogliaro, F.; Bearpark, M.; Heyd, J. J.; Brothers, E.; Kudin, K. N.; Staroverov, V. N.; Kobayashi, R.; Normand, J.; Raghavachari, K.; Rendell, A.; Burant, J. C.; Iyengar, S. S.; Tomasi, J.; Cossi, M.; Rega, N.; Millam, J. M.; Klene, M.; Knox, J. E.; Cross, J. B.; Bakken, V.; Adamo, C.; Jaramillo, J.; Gomperts, R.; Stratmann, R. E.; Yazyev, O.; Austin, A. J.; Cammi, R.; Pomelli, C.; Ochterski, J. W.; Martin, R. L.; Morokuma, K.; Zakrzewski, V. G.; Voth, G. A.; Salvador, P.; Dannenberg, J. J.; Dapprich, S.; Daniels, A. D.; Farkas, O.; Foresman, J. B.; Ortiz, J. V.; Cioslowski, J.; Fox, D. J. *Gaussian 09, Revision A.02*; Gaussian, Inc.: Wallingford, CT, 2009.
(43) Clark, T.; Alex, A.; Beck, B.; Burkhardt, F.; Chandrasekhar, J.; Gedeck, P.; Horn, A.; Hutter, M.; Martin, B.; Dral, P. O.; Rauhut, G.; Sauer, W.; Schindler, T.; Steinke, T.; *VAMP 11.0*; University of Erlangen, Germany, 2011.
(44) Imaginary frequencies of some noncovalent complexes below 16 cm^{-1} were ignored. See the Supporting Information for details.
(45) Chai, J.-D.; Head-Gordon, M. *Phys. Chem. Chem. Phys.* **2008**, *10*, 6615.
(46) Binkley, J. S.; Pople, J. A.; Hehre, W. J. *J. Am. Chem. Soc.* **1980**, *102*, 939.
(47) Binning, R. C., Jr.; Curtiss, L. A. *J. Comput. Chem.* **1990**, *11*, 1206.
(48) Blaudeau, J.-P.; McGrath, M. P.; Curtiss, L. A.; Radom, L. *J. Chem. Phys.* **1997**, *107*, 5016.
(49) Ditchfield, R.; Hehre, W. J.; Pople, J. A. *J. Chem. Phys.* **1971**, *54*, 724.
(50) Francl, M. M.; Pietro, W. J.; Hehre, W. J.; Binkley, J. S.; DeFrees, D. J.; Pople, J. A.; Gordon, M. S. *J. Chem. Phys.* **1982**, *77*, 3654.
(51) Gordon, M. S. *Chem. Phys. Lett.* **1980**, *76*, 163.
(52) Gordon, M. S.; Binkley, J. S.; Pople, J. A.; Pietro, W. J.; Hehre, W. J. *J. Am. Chem. Soc.* **1982**, *104*, 2797.
(53) Hariharan, P. C.; Pople, J. A. *Theor. Chem. Acc.* **1973**, *28*, 213.
(54) Hariharan, P. C.; Pople, J. A. *Mol. Phys.* **1974**, *27*, 209.
(55) Hehre, W. J.; Ditchfield, R.; Pople, J. A. *J. Chem. Phys.* **1972**, *56*, 2257.
(56) Rassolov, V. A.; Pople, J. A.; Ratner, M. A.; Windus, T. L. *J. Chem. Phys.* **1998**, *109*, 1223.
(57) Rassolov, V. A.; Ratner, M. A.; Pople, J. A.; Redfern, P. C.; Curtiss, L. A. *J. Comput. Chem.* **2001**, *22*, 976.
(58) Ciammaichella, A.; Dral, P. O.; Clark, T.; Tagliatesta, P.; Sekita, M.; Guldi, D. M. *Chem. Eur. J.* **2012**, Early view, DOI: 10.1002/chem.201202245.
(59) Schenker, S.; Schneider, C.; Tsogoeva, S. B.; Clark, T. *J. Chem. Theor. Comput.* **2011**, *7*, 3586.
(60) Lambert, C. *Angew. Chem., Int. Ed.* **2011**, *50*, 1756.
(61) Kamada, K.; Ohta, K.; Shimizu, A.; Kubo, T.; Kishi, R.; Takahashi, H.; Botek, E.; Champagne, B.; Nakano, M. *J. Phys. Chem. Lett.* **2010**, *1*, 937.
(62) Stewart, J. J. P. *J. Mol. Model.* **2007**, *13*, 1173−1213.
(63) Dral, P. O.; Clark, T. *J. Phys. Chem. A* **2011**, *115*, 11303.
(64) Pulay, P. *Chem. Phys. Lett.* **1980**, *73*, 393.
(65) Dewar, M.; Thiel, W. *J. Am. Chem. Soc.* **1997**, *99*, 4899.
(66) Dewar, M. J. S.; McKee, M. L.; Rzepa, H. S. *J. Am. Chem. Soc.* **1978**, *100*, 3607.
(67) Dewar, M. J. S.; Zoebisch, E. G.; Healy, E. F.; Stewart, J. J. P. *J. Am. Chem. Soc.* **1985**, *107*, 3902.
(68) Dewar, M. J. S.; Reynolds, C. H. *J. Comput. Chem.* **1986**, *7*, 140.
(69) Davis, L. P.; Guidry, R. M.; Williams, J. R.; Dewar, M. J. S.; Rzepa, H. S. *J. Comput. Chem.* **1981**, *2*, 433.
(70) Winget, P.; Clark, T. *J. Mol. Model.* **2005**, *11*, 439.
(71) Winget, P.; Horn, A. H. C.; Selçuki, C.; Martin, B.; Clark, T. *J. Mol. Model.* **2003**, *9*, 408.
(72) Materials Studio v6.0.0 ed.; Accelrys Software Inc.: 2011.
(73) Lee, C.; Yang, W.; Parr, R. G. *Phys. Rev. B* **1988**, *37*, 785.
(74) Miehlich, B.; Savin, A.; Stoll, H.; Preuss, H. *Chem. Phys. Lett.* **1989**, *157*, 200.
(75) Handy, N. C.; Cohen, A. J. *Mol. Phys.* **2001**, *99*, 403.
(76) Hoe, W.-M.; Cohen, A.; Handy, N. C. *Chem. Phys. Lett.* **2001**, *341*, 319.
(77) Clark, T.; Chandrasekhar, J.; Spitznagel, G. W.; Schleyer, P. V. *J. Comput. Chem.* **1983**, *4*, 294.
(78) Frisch, M. J.; Pople, J. A.; Binkley, J. S. *J. Chem. Phys.* **1984**, *80*, 3265.
(79) Hashimoto, S.; Seki, K.; Sato, N.; Inokuchi, H. *J. Chem. Phys.* **1982**, *76*, 163.
(80) Salinas, M.; Jäger, C. M.; Amin, A. Y.; Dral, P. O.; Meyer-Friedrichsen, T.; Hirsch, A.; Clark, T.; Halik, M. *J. Am. Chem. Soc.* **2012**, *134*, 12648.
(81) Dral, P. O.; Shubina, T. E.; Hirsch, A.; Clark, T. *ChemPhysChem* **2011**, *12*, 2581.
(82) Bauernschmitt, R.; Ahlrichs, R. *Chem. Phys. Lett.* **1996**, *256*, 454.
(83) Casida, M. E.; Jamorski, C.; Casida, K. C.; Salahub, D. R. *J. Chem. Phys.* **1998**, *108*, 4439.
(84) Furche, F.; Ahlrichs, R. *J. Chem. Phys.* **2002**, *117*, 7433.
(85) Furche, F.; Ahlrichs, R. *J. Chem. Phys.* **2002**, *117*, 7433.
(86) Scalmani, G.; Frisch, M. J.; Mennucci, B.; Tomasi, J.; Cammi, R.; Barone, V. *J. Chem. Phys.* **2006**, 124.

(87) Scalmani, G.; Frisch, M. J.; Mennucci, B.; Tomasi, J.; Cammi, R.; Barone, V. *J. Chem. Phys.* **2006**, 124.
(88) Stratmann, R. E.; Scuseria, G. E.; Frisch, M. J. *J. Chem. Phys.* **1998**, *109*, 8218.
(89) Van Caillie, C.; Amos, R. D. *Chem. Phys. Lett.* **1999**, *308*, 249.
(90) Van Caillie, C.; Amos, R. D. *Chem. Phys. Lett.* **2000**, *317*, 159.
(91) Becke, A. D. *J. Chem. Phys.* **1993**, *98*, 5648.
(92) Hill, I. G.; Kahn, A.; Soos, Z. G.; Pascal, R. A. *Chem. Phys. Lett.* **2000**, *327*, 181.
(93) Djurovich, P. I.; Mayo, E. I.; Forrest, S. R.; Thompson, M. E. *Org. Electron.* **2009**, *10*, 515.
(94) Cappellini, G.; Malloci, G.; Mulas, G. *Superlattices Microstruct.* **2009**, *46*, 14.
(95) Nayak, P. K.; Periasamy, N. *Org. Electron.* **2009**, *10*, 1396.
(96) Sharifzadeh, S.; Biller, A.; Kronik, L.; Neaton, J. B. *Phys. Rev. B* **2012**, 85.
(97) Hummer, K.; Ambrosch-Draxl, C. *Phys. Rev. B* **2005**, 71.
(98) Konarev, D. V.; Kovalevsky, A. Y.; Litvinov, A. L.; Drichko, N. V.; Tarasov, B. P.; Coppens, P.; Lyubovskaya, R. N. *J. Solid State Chem.* **2002**, *168*, 474.
(99) Zhurko, G. A.; Zhurko, D. A. Chemcraft 1.6 (Build 355); 2012.
(100) Rauhut, G.; Clark, T.; Steinke, T. *J. Am. Chem. Soc.* **1993**, *115*, 9174.
(101) Schleyer, P. V.; Jiao, H. J.; Hommes, N. J. R. V.; Malkin, V. G.; Malkina, O. L. *J. Am. Chem. Soc.* **1997**, *119*, 12669.
(102) Schleyer, P. v. R.; Maerker, C.; Dransfeld, A.; Jiao, H. J.; Hommes, N. J. R. V. *J. Am. Chem. Soc.* **1996**, *118*, 6317.
(103) Chen, Z. F.; Wannere, C. S.; Corminboeuf, C.; Puchta, R.; Schleyer, P. V. *Chem. Rev.* **2005**, *105*, 3842.
(104) Cheeseman, J. R.; Trucks, G. W.; Keith, T. A.; Frisch, M. J. *J. Chem. Phys.* **1996**, *104*, 5497.
(105) Ditchfield, R. *Mol. Phys.* **1974**, *27*, 789.
(106) Ruud, K.; Helgaker, T.; Bak, K. L.; Jorgensen, P.; Jensen, H. J. A. *J. Chem. Phys.* **1993**, *99*, 3847.
(107) Wolinski, K.; Hinton, J. F.; Pulay, P. *J. Am. Chem. Soc.* **1990**, *112*, 8251.
(108) London, F. *J. Phys. Radium* **1937**, *8*, 397.
(109) McWeeny, R. *Phys. Rev.* **1962**, *126*, 1028.
(110) Clar, E. *The Aromatic Sextet*; Wiley: London, 1972.
(111) Cremer, D.; Günther, H. *Liebigs Ann. Chem.* **1972**, *763*, 87.
(112) Moran, D.; Stahl, F.; Bettinger, H. F.; Schaefer, H. F.; Schleyer, P. v. R. *J. Am. Chem. Soc.* **2003**, *125*, 6746.